

**An Endotracheal Aerosolization Device for Laboratory Investigation of  
Nanoparticle Suspension Pulmonary Delivery: *in Vitro* and *in Vivo* Validation**

Zhengwei **Huang**<sup>a</sup>, Ying **Huang**<sup>a,\*</sup>, Cheng **Ma**<sup>a</sup>, Xiangyu **Ma**<sup>b</sup>, Xuejuan **Zhang**<sup>a,c</sup>, Ling **Lin**<sup>a</sup>,

Ziyu **Zhao**<sup>a</sup>, Xin **Pan**<sup>a,\*\*</sup>, Chuanbin **Wu**<sup>a</sup>

<sup>a</sup> School of Pharmaceutical Sciences, Sun Yat-Sen University, Guangzhou 510006, Guangdong,  
P. R. China

<sup>b</sup> College of Pharmacy, The University of Texas at Austin, Austin, TX 78712, USA

<sup>c</sup> Institute for Biomedical and Pharmaceutical Sciences, Guangdong University of Technology,  
Guangzhou, 510006, P.R. China

\* and \*\* are corresponding authors.

## **Supplementary material**

## 1 Determination of $DL_{SLN}$ , $EE_{SLN}$ , $DL_{SLNS}$ and $EE_{SLNS}$

Drug loading (DL) and encapsulation efficiency (EE) of SLNS formulations were determined via ultrafiltration cells. The cut-off molecular weight of ultrafiltration cells was 30000. The procedures were as follow. For determination of  $DL_{SLN}$  and  $EE_{SLN}$ , 1 mL of BUD or P4 loaded SLNS formulation was placed in an ultrafiltration cell, and subjected to centrifugation at 10000 rpm for 20 min (DL-4000B, Anting Scientific Instrument Factory, Shanghai, China). The residual solid was dissolved by a proper volume of hot acetonitrile (about 70°C). Meanwhile, 1 mL SLNS formulation was freeze-dried and the residues were precisely weighed. For determination of  $DL_{SLNS}$  and  $EE_{SLNS}$ , 1 mL sample was directly dissolved by a proper volume of acetonitrile at 70°C. Sample dissolving was finished within a sealed-container to avoid evaporation of acetonitrile. The formulation-dissolving systems were filtered through 0.22  $\mu\text{m}$  nylon-66 membrane and then assayed by HPLC-UV. The parameters  $DL_{SLN}$ ,  $EE_{SLN}$ ,  $DL_{SLNS}$  and  $EE_{SLNS}$  could be calculated according to **Eq. S1~S4**:

$$DL_{SLN} (\%) = \frac{\text{Determined cargo amount}}{\text{Weight of the sample}} \times 100\% \quad \text{Eq. S1}$$

$$EE_{SLN} (\%) = \frac{DL_{SLN}}{\text{Theoretical DL of suspending nanoparticles}} \times 100\% \quad \text{Eq. S2}$$

$$DL_{SLNS} (\mu\text{g/mL}) = \frac{\text{Determined cargo amount}}{\text{Volume of the sample}} \quad \text{Eq. S3}$$

$$EE_{SLNS} (\%) = \frac{DL_{SLNS}}{\text{Theoretical DL of entire SLNS formulation}} \times 100\% \quad \text{Eq. S4}$$

## 2 Gelation phenomenon of SLNS formulations

Gelation phenomenon, an irreversible lipid aggregation process, was often observed in SLNS. The mechanism underlying this phenomenon was still unclear, but there were strategies to avoid it. Removal of impurities was regarded as a critical method by the authors, and thus pretreatment of

PP was carried out. Illustrated by **Fig. S1**, gelation phenomenon was not witnessed in PP after pretreatment while took place occasionally (about 1 in 5 batches) in PP without pretreatment. This confirmed the effectiveness of pretreatment.

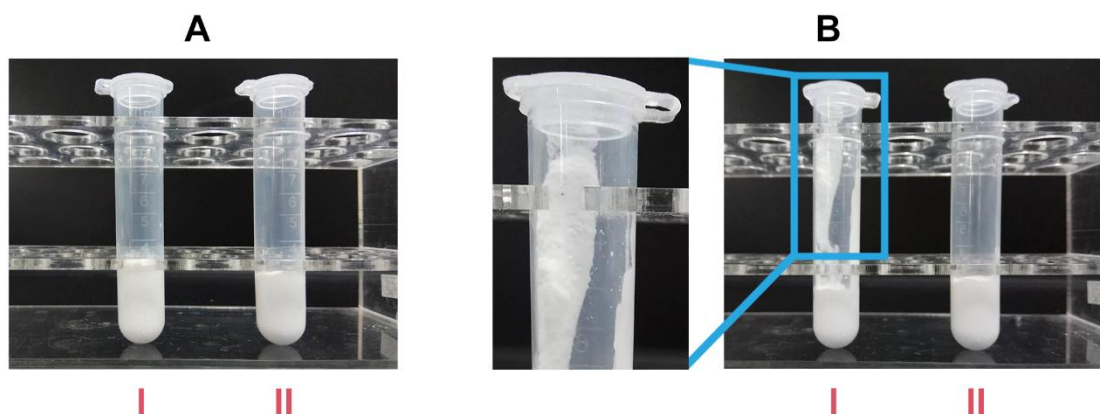


**Fig. S1** Typical images about gelation phenomenon. (A) SLNS prepared from PP after pretreatment. I: sample after manually shaking for 10 times; II: unshaken sample. (B) SLNS prepared from PP without pretreatment. I: sample after manually shaking for 10 times; II: unshaken sample.

### 3 Graphical interpretation of the influence of aerosolization on various properties

According to **Fig. 5** and **Fig. 6**, the particle size, PDI, ZP,  $DL_{SLN}$ ,  $EE_{SLN}$ ,  $DL_{SLNS}$ ,  $EE_{SLNS}$ , fluorescence spectrum and peak fluorescence intensity before and after *in vitro* aerosolization did not markedly alter. A graphical summary is depicted by **Fig. S2**.

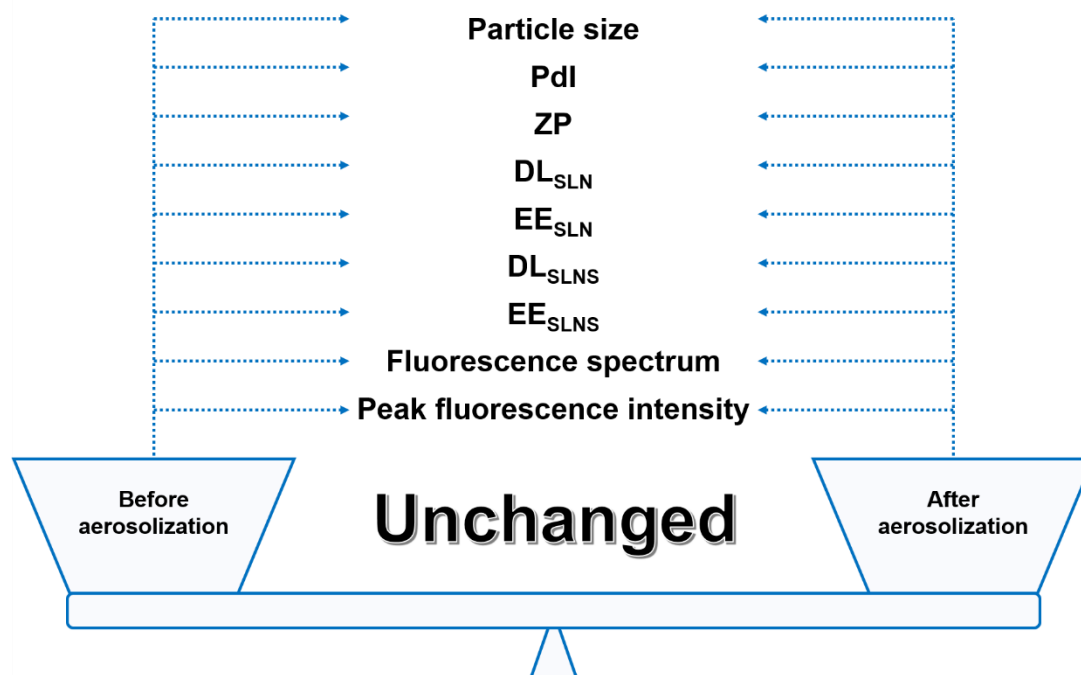


**Fig. S2** A graphical interpretation of the influence of aerosolization on various properties.

Abbreviations: Pdl: polydispersity index; ZP: zeta-potential; DL<sub>SLN</sub>: drug loading of the suspending nanoparticles; EE<sub>SLN</sub>: encapsulation efficiency of the suspending nanoparticles; DL<sub>SLNS</sub>: drug loading of the entire SLNS formulations; EE<sub>SLNS</sub>: encapsulation efficiency of the entire SLNS formulations.

#### **4 Validation of HPLC-UV methods for pulmonary BUD concentration quantification**

The HPLC-UV method for lung samples was validated, and the results are summarized in **Tab. S1** and **S2**.

**Tab. S1** Results of the precision and accuracy of HPLC-UV method.

Group	No.	Theoretical concentration (ng/mL)	Determined concentration (ng/mL)	Accuracy (%)	Mean (%)	RSD (%)
L	1	65	58.05	89.31	93.28	3.46
	2	65	59.68	91.81		
	3	65	60.50	93.07		
	4	65	63.76	98.09		
	5	65	61.18	94.12		
M	1	143	142.23	99.46	96.20	5.09
	2	143	125.28	87.61		
	3	143	140.55	98.29		
	4	143	141.29	98.81		
	5	143	138.45	96.82		
H	1	260	237.55	91.36	92.53	1.79
	2	260	238.52	91.74		
	3	260	240.83	92.63		
	4	260	247.93	95.36		
	5	260	238.01	91.54		

**Tab. S2** Results of the recovery of HPLC-UV method.

Group	No.	Spiked concentration (ng/mL)	Recovered concentration (ng/mL)	Recovery (%)	Mean (%)	RSD (%)
L	1	65	59.55	91.62	89.37	6.32
	2	65	63.40	97.53		
	3	65	55.66	85.63		
	4	65	57.97	89.19		
	5	65	53.88	82.89		
M	1	143	139.18	99.33	98.49	2.08
	2	143	140.32	98.13		
	3	143	138.78	97.05		
	4	143	145.95	102.06		
	5	143	139.95	97.87		
H	1	260	242.42	93.24	93.86	2.45
	2	260	243.58	93.69		
	3	260	235.95	90.75		
	4	260	252.57	97.14		
	5	260	245.61	94.47		

### 5 Fluorescence spectra of P4

P4 was a self-synthesized ACQ fluorescence probe. The fluorescence spectra of P4 were recorded within the range of 645~660 nm for excitation wavelength and 200~900 nm for emission wavelength (**Fig. S3**). It was revealed that 651 nm was the maximum excitation wavelength ( $\lambda_{ex}$ ) and 673 nm was the maximum emission wavelength ( $\lambda_{em}$ ).

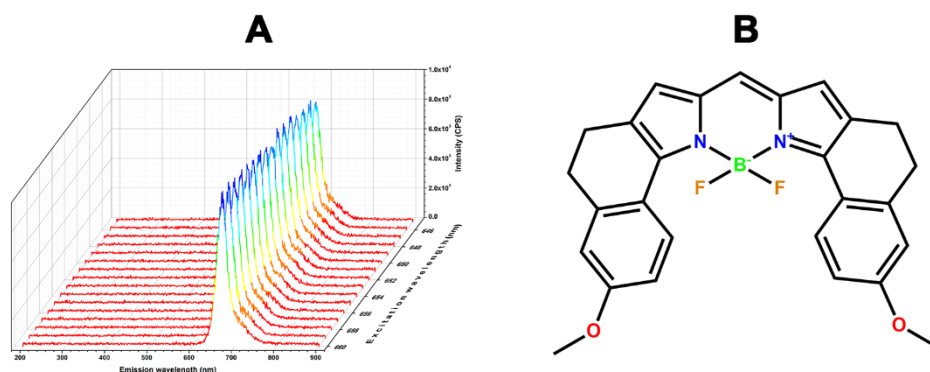


**Fig. S3** (A) Fluorescence spectra of P4 (excitation wavelength: 645~660 nm; emission wavelength: 200~900 nm); (B) The molecular structure of P4.

#### 6 *In vivo* bioimaging of the SD rats before administration

The photographs of SD rats before administration were shown in **Fig. S4**. The maximum of fluorescence signal was c.a. 3400 CPS.

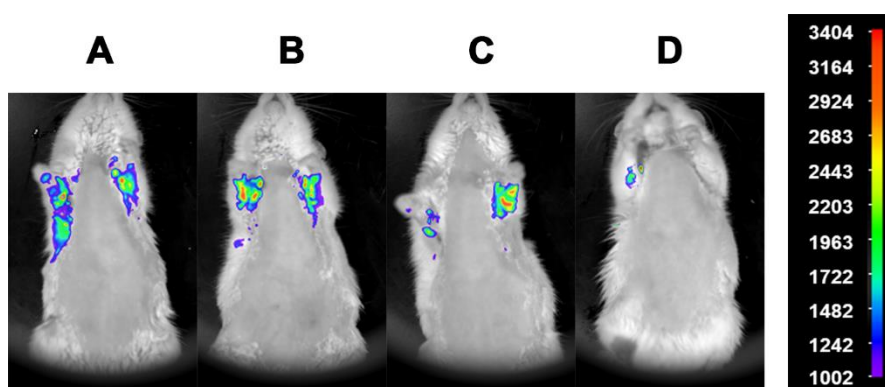


**Fig. 4** Typical images taken in the *in vivo* bioimaging. The photograph of SD rats to be administrated by P4-SLNS1~4 was A~D, respectively.

## 7 *Ex vivo* bioimaging

The *ex vivo* bioimaging results is provided in **Fig. S5**. It could be found that fluorescence signal was located in the lung region, and the maximum signal intensity was proportional to the DL and EE of the SLNS. Of note, there were some differences in the operating parameters between *in vivo* bioimaging and *ex vivo* bioimaging: exposure time 0.25 s for *in vivo* bioimaging and 0.10 s for *ex vivo* bioimaging, high gain (feedback) for *in vivo* imaging and low gain (feedback) for *ex vivo* imaging. Due to that the muscle, skin, bone and other tissues would undermine the fluorescence emitted by P4 in SD rats, the fluorescence signal detected in *in vivo* bioimaging was remarkably lower than that in *ex vivo* bioimaging. Thus, a longer exposure time and higher feedback was selected in *in vivo* bioimaging.

The overall fluorescence signal of a, b, c, d, e was  $9.93 \times 10^{10}$ ,  $6.60 \times 10^{10}$  ph/s,  $6.63 \times 10^8$  ph/s, ph/s  $7.15 \times 10^{10}$  ph/s and 0 ph/s, respectively. The area-normalized fluorescence signal of them was  $7.79 \times 10^8$  ph/(s·mm<sup>2</sup>),  $6.75 \times 10^8$  ph/(s·mm<sup>2</sup>),  $6.46 \times 10^8$  ph/(s·mm<sup>2</sup>),  $4.48 \times 10^8$  ph/(s·mm<sup>2</sup>) and 0 ph/(s·mm<sup>2</sup>), respectively. The results were in accordance with the *in vivo* bioimaging.

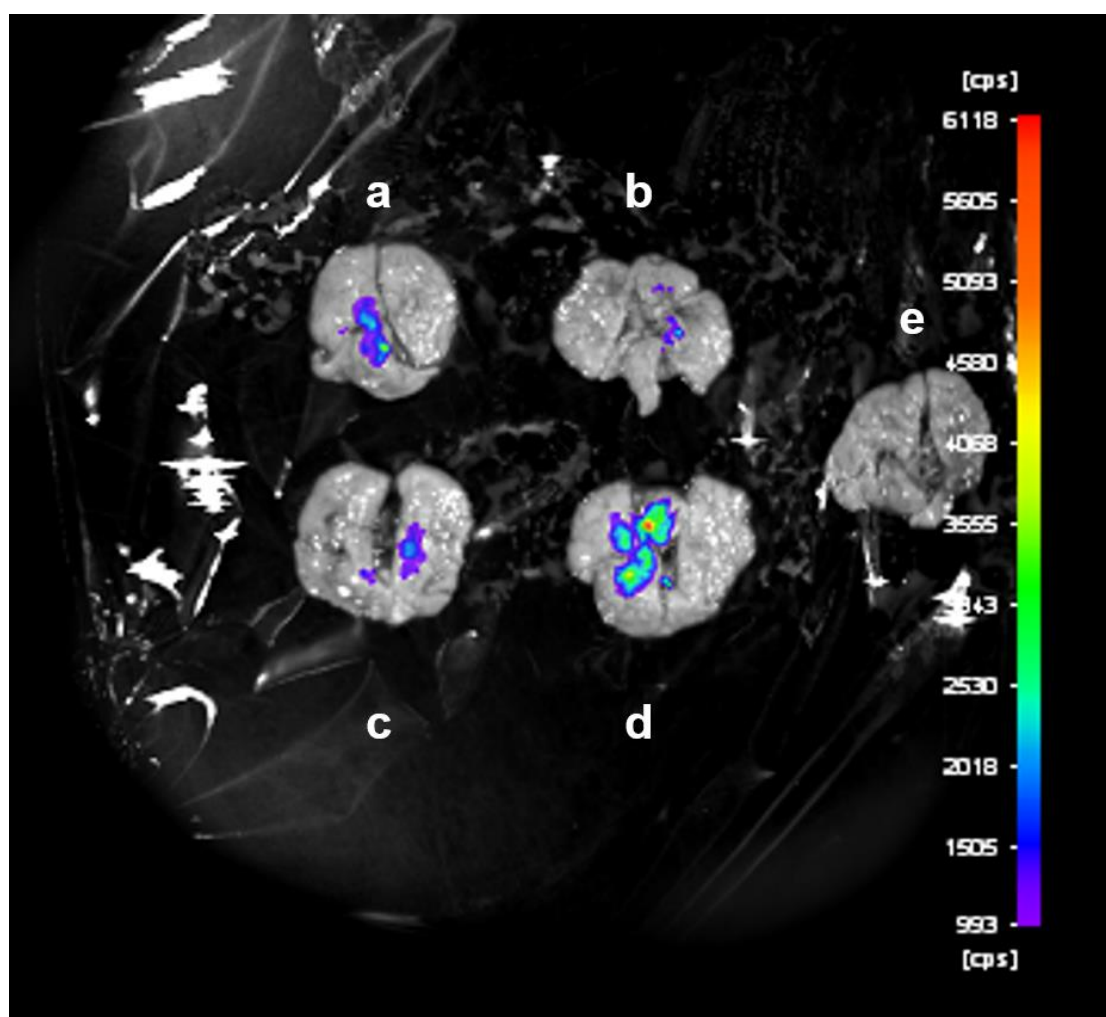


**Fig. S5** Typical images taken in the *ex vivo* bioimaging of the lungs of SD rats. (a) the lung of the SD rat administrated by P4-SLNS4; (b) the lung of the SD rat administrated by P4-SLNS3; (c) the lung of the SD rat administrated by P4-SLNS2; (d) the lung of the SD rat administrated by P4-SLNS1; (e) the lung of the SD rat not administrated (blank).